8-2018

Novel Detection and Analysis using Deep Variational Autoencoders

Tucker B. Graydon
tbg8514@rit.edu

Novel Detection and Analysis using Deep Variational Autoencoders

by

Tucker B. Graydon

A Thesis Submitted in Partial Fulfillment of the Requirements for the
Degree of Master of Science in Electrical and Microelectronic Engineering

Supervised by

Professor Dr. Ferat Sahin
Department of Electrical and Microelectronic Engineering
Kate Gleason College of Engineering
Rochester Institute of Technology
Rochester, New York
August 2018

Approved by:

Dr. Ferat Sahin, Professor
Thesis Advisor, Department of Electrical and Microelectronic Engineering

---

Dr. Sohail Dianat, Professor
Committee Member, Department of Electrical and Microelectronic Engineering

---

Dr. Ahmet Okutan, Professor
Committee Member, Department of Electrical and Microelectronic Engineering

Thesis Release Permission Form

Rochester Institute of Technology
Kate Gleason College of Engineering

Title:

Novel Detection and Analysis using Deep Variational Autoencoders

I, Tucker B. Graydon, hereby grant permission to the Wallace Memorial Library to reproduce my thesis in whole or part.

Tucker B. Graydon

Date

To my family, friends and colleagues.

Acknowledgments

Throughout my undergraduate and graduate studies here at RIT, there are many who deserve my gratitude.

Foremost, I must thank Dr. Ferat Sahin. You have been a constant source of advice and wisdom for me and it is through your guidance and encouragement that I am here today.

Shitij, you have been there at all hours of the day and night supporting me and engaging in long conversations that pushed my work further ahead. You are truly a good mentor and good friend.

Ryan, I have known you in many capacities over the years. In them all, you always provided me with invaluable perspective and counsel, which has made me a better engineer. This work would not have been possible without your influence.

Celal, you have always been the never-ending optimist in our lab, keeping us going even at 2am the day before finals.

Last, I would like to say thank you to Sadie, your support through countless long nights and difficult semesters made it all worth it.

For the rest not mentioned **I** thank you **all**.

Abstract

Novel Detection and Analysis using Deep Variational Autoencoders

Tucker B. Graydon

Supervising Professor: Dr. Ferat Sahin

This paper presents a Novel Identification System which uses generative modeling techniques and Gaussian Mixture Models (GMMs) to identify the main process variables involved in a novel event from multivariate data. Features are generated and subsequently dimensionally reduced by using a Variational Autoencoder (VAE) supplemented by a denoising criterion and a β disentangling method. The GMM parameters are learned using the Expectation Maximization(EM) algorithm on features collected from only normal operating conditions. A one-class classification is achieved by thresholding the likelihoods by a statistically derived value. The Novel Identification method is verified as a detection method on existing Radio Frequency (RF) Generators and standard classification datasets. The RF dataset contains 2 different models of generators with almost 100 unique units tested. Novel Detection on these generators achieved an average testing true positive rate of 97.31% with an overall target class accuracy of 98.16%. A second application has the network evaluate process variables of the RF generators when a novel event is detected. This is achieved by using the VAE decoding layers to map the GMM parameters back to a space equivalent to the original input, resulting in a way to directly estimate the process variables fitness.

List of Contributions

- T. Graydon, F. Sahin, "Novel Detection and Analysis using β-DVAE Networks," *Systems, Man and Cybernetics (SMC), 2018 IEEE International Conference*, 2018. Accepted for publication.

Contents

List of Figures

List of Tables

Chapter 1

Introduction

Current systems in the Integrated Circuit (IC) manufacturing and fabrication industry depend on the reliability and availability of the process equipment. Any failures of process machinery mean down time, ruined products, resources lost, and an overall increase in the cost of ownership for the company. Tools such as RF plasma generators are critical in the IC fabrication process. In order to maximize production and minimize cost of ownership, the reliability and operation of these components is critical. There are currently tools available to monitor system health, however the ability to analyze the symptoms of the failure can dramatically shorten machine down time, keeping cost of ownership low.

Novel event detection, specifically fault detection and identification are a derivative of statistical process control. In recent years it has been shown that the addition of machine learning leads to better fault detection [3]. Current fault detection methods are based on modeling a system and detecting deviations from a model of a *normal* system. Previous work has been done with regard to modeling systems and classifying operations as *normal* or *not-normal*. Gaussian Mixture Models [4] [2] [5], Support Vector Machines (SVM) [6], Radial Basis Function Networks (RBFN) [7][8], Deep Autoencoders [9] and Novelty Detection have been explored by Bowen et al. and Chandreshekar et al. Their work on a

modified Novelty Detection Framework (NDF) has been an inspiration for the work presented in this paper. The results of the NDF as well as Bowen's embedded application validate the additional need for an initial report analyzing the fault event at the input level.

This novelty analysis methodology will attempt to utilize previous one-class classification methods along with generative neural network architectures in order to detect a novel event as well as relate the learned one-class classifier parameters back to the original process variables. By relating the classification model back to the input space the fitness of each process variable can be estimated and can be used to reduce the down time of the system.

This paper outlines the use of β-Disentangling, Denoising Variational Autoencoders (β-DVAE) with a GMM one-class classifier as a fault detection and analysis system for RF plasma generators. The remainder of this paper will follow this outline: Section II defines β-DVAE and GMM, Section III explains the proposed method in detail, and Section IV summarizes the experimental results.

Chapter 2

Background Literature

One-Class Classification

The basis of machine learning is that a set of data which represents some parameters or features of a system where all possible inputs and outputs are uniformly represented. This is labeled as the training set of data. In the field of fault analysis and detection there is no practical way of obtaining faulty data from all possible modes of fault or failure. It is more common that there exists significant data of the desired mode of operation. Typically, fault analysis methods utilize multi-class classifiers, in these multi-class situations machine learning methods such as support vector machines, neural networks, radial basis functions and Bayesian networks are used. Typical machine learning methods rely on the availability of data for training the models. Therefore, the machine learning methods can only be as successful as the data available during training. For multi-class methods both the target and non-target class data must be available. There is a common difficulty in collecting data from non-target classes, specifically non-normal operation modes. Since there is an immense difficulty associated with collecting reliable data from *every possible mode of failure* there has been a paradigm shift towards learning only the normal modes of operation for a system rather than attempting to differentiate non-normal from the normal modes.

The assumption of one-class classification is that information is only available from one class, the target class. The problem one-class classification poses is defining a boundary around the target class in order to maximize target acceptance and minimize non-target acceptance. The two most popular one-class realizations are density based and boundary based approaches. Density based methods estimate the densities of the training data and determine threshold values. Estimating the densities can be accomplished using many different distributions such as Gaussian, Poisson, Bernoulli and mixtures of these. Density based methods can be very effective as long as there is sufficiently large training data and a proper model is applied. In the case of limited training samples, density based methods will not generalize the data appropriately. It is therefore appropriate to solve the problem with the available data and use boundary methods to separate the target data. The commonly used boundary based methods include k-means, k nearest neighbor (KNN), and support vector data description (SVDD). These boundary based methods are capable of working on small dataset sizes but are heavily reliant on distance measures and very sensitive to feature scaling.

Mixture Models

Mixtures of distributions are commonly used as mathematical methods for statistical modeling of a set of data. Mixture models have been applied as clustering and latent class analysis and are generally favored for their ability to provide descriptive models for a data distribution. A typical mixture model with regards to clustering assumes a set of $N \times M$

dimensional data can be represented as a finite number of K components, with some unknown proportions.

The general formulation of a mixture model is as follows: An observed random variable is denoted as $y_1, ..., y_N$ such that y_j is a random vector with probability density function $f(y_j) \in \mathbb{R}^M$ and $j = 1, ..., N$. Therefore y_j contains M measurements of the jth observed sample of random variables and $Y = (y_1^T, ...y_N^T)^T$ contains all observed samples. The probability density function of an observed random variable, in parametric form for a K-component mixture is:

$$f(y_j; \Psi) = \sum_{i=1}^{K} \pi_i f_i(y_j; \theta_i) \tag{2.1}$$

The Ψ term here represents any unknown parameters of the mixture model and can be expressed below, where a ξ term is used to represent all *a priori* parameters in θ.

$$\Psi = (\pi_1, ..., \pi_K, \xi^T)^T \tag{2.2}$$

Letting $\pi = (\pi_1, ..., \pi^T)^T$ be a vector of mixing weights where $\sum_{i=1}^{K} \pi_i = 1$. Equation 2.1 is the general form of a mixture model. For the complete realization, a distribution must be assumed in place of $f(\times)$, the most frequently used being the Gaussian distribution.

Gaussian Mixture Models

The Gaussian Mixture model is a mixture model that assumes data is approximately Gaussian distributed.

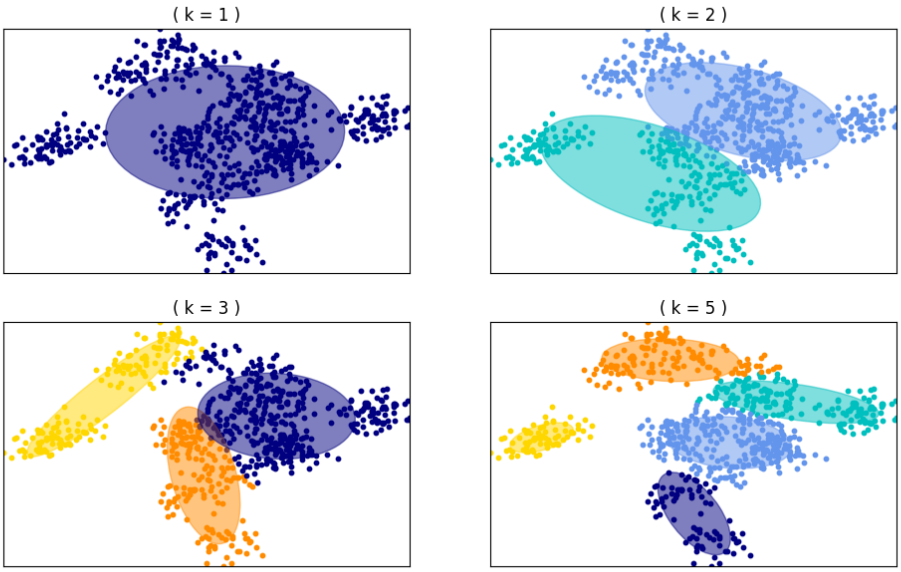

Figure 2.1: The selection of k centroids is key for fitting the data. A low k may cause an overgeneralized model and a high value will lead to overfitting.

A Gaussian Mixture Model is defined as a combination of k combinations of Gaussian densities. A Gaussian density in d-dimensional space is characterized by a mean $\mu \in \mathbb{R}^d$ and a $d \times d$ covariance matrix Σ [10][11]. The Gaussian density function is then defined as:

$$g(x|\mu, \Sigma) = (2\pi)^{-d/2}|\Sigma|^{-1/2}exp\Big(-\frac{1}{2}(x-\mu)^T\Sigma^{-1}(x-\mu)\Big) \tag{2.3}$$

A k component Gaussian mixture is defined by:

$$p(x) = \sum_{i=1}^{k} \pi_i g(x|\mu_i, \Sigma_i) \tag{2.4}$$

Where π_i are weight values for each mixture and $g(x|\mu_i, \Sigma_i)$ is the i^{th} mixture density. The weighted densities are summed into a Gaussian mixture model. The target class and outliers can then be identified by thresholding the calculated Gaussian likelihoods where μ and σ are the mean and standard deviation of the training data's log-likelihood values.

$$\mathcal{L}_{th} = \mu_{\mathcal{L}} - \lambda \sqrt{\sigma_{\mathcal{L}}} \tag{2.5}$$

There are two popular methods for learning the parameters of the mixture models, Expectation Maximization (EM) and Variational Bayesian Inference. The EM algorithm is an iterative process used to calculate the maximum likelihood estimation (MLE) with missing or unknown data. An iteration of EM is comprised of two steps, an expectation step followed by a maximization step. In the expectation step, the unknown or missing data is estimated with respect to the observed data and the current estimates of the model parameters. Then the maximization step maximizes the likelihood of the data with the assumption that the missing data is known. This process iterates until the model parameters converge.

Generative Modeling

The goals of generative modeling are two-fold: (1) Learn a latent representation of a complex, high dimension dataset to encourage higher cluster/class separation and (2) Learn

a model to generate accurate samples from the latent variables. When applied with one-class classification the generative model encodes the data to latent representations for easier classification [12] and can scale a model learned in the latent space to the input space. The remainder of this section defines variational autoencoders, the denoising criterion, β-VAE and GMMs for one-class classification.

The traditional autoencoder architecture has been utilized since the 1980's as a method for linear and non-linear dimension reduction. The fundamental principle of the autoencoder is the bottleneck design where an input is mapped down to a lower dimension and then remapped to reconstruct the ordinal data. This mapped latent variable set is commonly used for training machine learning models in a less computationally intensive space. However, the networks's ability to apply non-linear mappings is limited to the non-linear activation functions applied in the hidden layers. Utilizing activations such as *sigmoid* or *tanh* allow for non-linearities in the mapping but significantly increase the risks of diminishing gradients in larger networks.

There have been attempts to increase the flexibility and strength of the autoencoders latent variable mappings. Denoising criteria, sparsity and contractive penalties, as well as stochastic parameterizations of layer weights have been applied to create more salient and unique latent variables. This push for better encoding of high dimension data has also been spurred on by growing interest in the field of generative models and deep learning. These new methodologies learn to map the inputs to latent dimensions and then attempt to sample the latent variables in order to generate artificial output images.

Autoencoders

Some of the generative modeling architectures discussed above exploit a particular type of neural network, an auto-associator, this is also called an autoencoder or a Diabolo network. There are also connections between the autoencoder and Restricted Bolzman Machines (RBM). Because of the simplicity of training a shallow autoencoder network they have long been used to initialize larger networks or to aid in the training of much deeper networks where each layer has an associated autoencoder that can be trained separately.

An autoencoder is trained to encode an input in some representation such that the input can be reconstructed from that representation. Therefore the target is the input itself. If a single hidden linear layer and a mean squared error is used as a criterion for training the network, the k hidden units learn a projection of the data into the k principal components of the data. This architecture converges to match principal component analysis (PCA) projections. Changing the hidden layer to a non-linear function causes the network to behave very differently from standard PCA and kernel PCA with a non-linear kernel. This non-linearity allows the network to capture multi-modal aspects of the input distribution. The most common generalization of this design switches the mean squared error for minimizing a negative log-likelihood of reconstructing the input:

$$\mathcal{L}_{RE} = -\log P(x|c(x)) \tag{2.6}$$

where $c(x)$ is the encoding function of the network. The main goal is that $c(x)$ is a

distributed representation that captures the main factors of variation in the data.

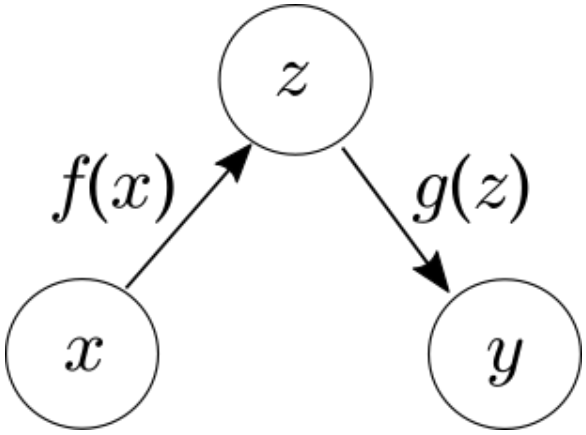

Figure 2.2: A Standard Autoencoder Layout

There is a large risk in the design of these networks. Given there are no other constraints on the system, an n-dimensional input and a hidden layer with a size greater than n has the potential to learn the input exactly, learning the identity function for the mapping. It has been disputed introducing constraints such as early stopping and $L2$ regularization with stochastic gradient descent can allow an over-complete hidden layer to learn useful representations, however this still introduces more constraints than just an over-complete layer and is beyond the scope of this research. Instead, or in addition to adding regularization to the network, one strategy is to incite marginal noise in the encodings which will be discussed in later sections. Other methods used to force the autoencoder to learn useful representations include imposing a sparsity constraint on the reconstruction/loss criterion, as well as introducing stochastic layers rather than the typical hidden layers.

Denoising Criterion

One of the central objectives of machine learning is the ability to generalize new configurations of observable variables from training data. In the most general sense this means determining how to redistribute the probability density associated with each training example from the empirical distribution. One approach to achieving this goal is through manifold learning which is attempting to model an embedded lower dimensional manifold that the high dimension data originates from. Parzan density estimation and principal component analysis (PCA) have been used for this in the past, however they suffer from isotropic variances or are limited to only linear manifolds. In a majority of manifold learning methods, the local shapes for the manifold are defined by a basis indicating the plausible directions of variation, i.e. a tangent plane to the point on the manifold. Most methods then diverge on how to combine these local tangential planes along the manifold in order to model the global manifold structure or density. The focus on local generalizations for these methods leads to issues with erratic manifolds that have many peaks and valleys. This correlates with the curse of dimensionality where, in order to learn the global manifold, the required training examples increases exponentially with manifold complexity. Recently non-linear, non-locally generalizing manifold learning methods have been produced using deep learning methods such as autoencoders. Denoising and contractive autoencoders (DAE, CAE) have great promise as manifold learning methods that can achieve local generalization without being restricted to local learning.

The approach of both the denoising autoencoder and the contractive autoencoder relate

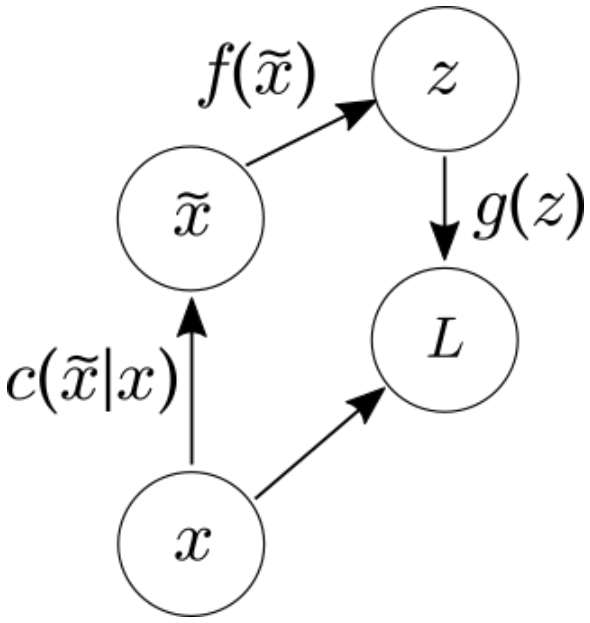

Figure 2.3: The denoising criterion modifies a typical autoencoder by adding a stochastic mapping layer to locally corrupt an input.

by either physically varying the training data locally with corruption, or by adding a penalizing term targeting local variances. The contractive autoencoder modifies the objective function of traditional autoencoders by adding the Frobenius norm of the Jacobian of the input and the latent encoding. This regularizing term penalizes the sensitivity of the input features to local variances. The denoising approach corrupts an input random variable (x) using a known conditional distribution $C(\tilde{x}|x)$. The DAE is trained to estimate the reverse conditional $g(f(\tilde{x}))$ or $P(x|\tilde{x})$ in order to determine a consistent estimator of $P(X)$.

The typical autoencoder structure takes an input $x \in [-1, 1]^d$, and maps it to a hidden, latent representation $z \in [-1, 1]^{d'}$ by a deterministic mapping $z = f_\theta(x) = \mathbf{W}x + b$, parameterized by $\theta = \{\mathbf{W}, b\}$. Here $\mathbf{W}$ is a $d' \times d$ weight matrix and b is a bias vector. The z latent representation is then mapped back to a "reconstructed" output vector $y \in [-1, 1]^d$. This

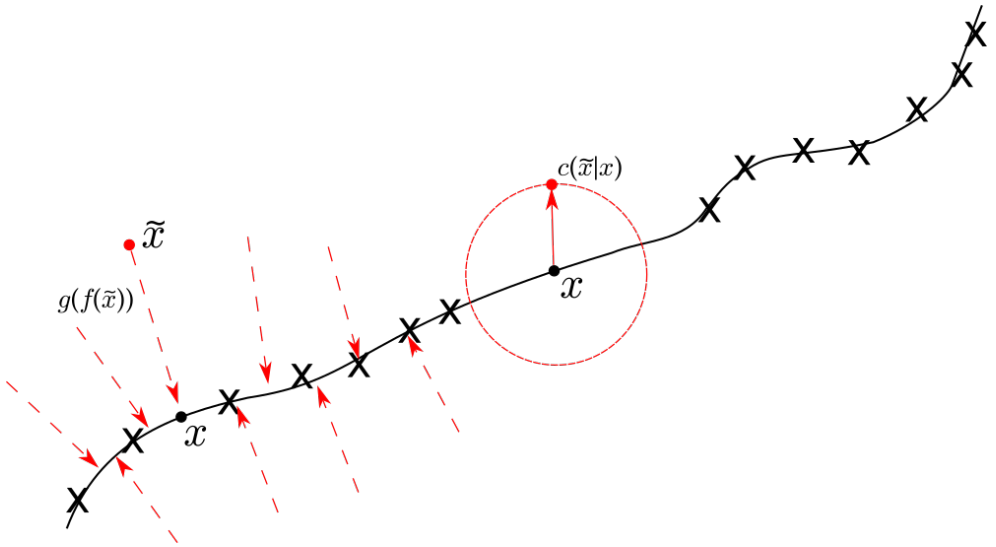

Figure 2.4: Corruption from a Manifold perspective. Assume data x is concentrated on a low dimension manifold. Corrupted examples are created by applying a corrupting process $C(\tilde{x}|x)$, these will lie further from the manifold. $g(f(\tilde{x}))$ is then used to project them back onto the manifold [1].

mapping is defined by $y = g_{\theta'}(z) = \mathbf{W}'z + b'$, with $\theta' = \{\mathbf{W}', b'\}$. The weight matrix $\mathbf{W}'$ of the reverse mapping can have additional constraints imposed such as $\mathbf{W}' = \mathbf{W}$, which is termed *tied-weights*. Using this method each input variable x is mapped to to a latent variable in z which is then reconstructed to y. The parameters of this model are optimized to minimize the average reconstruction error between x and y as shown in Eq. 2.7.

$$\theta^*, \theta'^* = \underset{\theta^*,\theta'^*}{\arg\min} \frac{1}{n} \sum_{i=1}^{n} L\left(x^i, z^i\right) = \underset{\theta^*,\theta'^*}{\arg\min} \frac{1}{n} \sum_{i=1}^{n} L\left(x^i, g_{\theta'}(f_\theta(x^i))\right) \tag{2.7}$$

Here L is any loss function such as squared error $L(x, y) = \|x - y\|^2$ or if the data can be considered analogous to bit vectors or probabilities, the cross-entropy loss (Eq. 2.8) may be used.

$$L_H(x, y) = -\sum_{k=1}^{d} \Big[x_k \log y_k + (1 - x_k) \log(1 - y_k) \Big] \tag{2.8}$$

The denoising criterion modifies the original autoencoder by corrupting the input data point and training the network to predict/reconstruct the original, uncorrupted input. The corruption process, defined as $C(\tilde{x}|x)$ represents the conditional distribution over the corrupted samples ($\tilde{x}$), given the original input x. By training an autoencoder with this new input the network is learning the reconstruction distribution, $P_{reconstruct}(x|\tilde{x})$.

In traditional autoencoders the addition of corruption to the input layer is commonly used to increase the encoding and decoding network's resilience to noise in the input data. VAEs with the denoising criterion can be trained similarly to the way denoising autoencoders are trained:

1. Sample an input with injected noise $\tilde{x} \sim p(\tilde{x}|x)$
2. Sample $z \sim q(z|\tilde{x})$ and
3. Sample the reconstructed data from the decoder network $p_\theta(x|z)$ [13][14].

Since the inference network has been modified by the injected noise the objective function is modified from the traditional VAE:

$$\mathcal{D}_{dvae}(\theta, \phi, x) = KL(\tilde{q}_\phi(z|\tilde{x}) || p_\theta(z)) \tag{2.9}$$

Variational Autoencoders

Autoencoding variational Bayes was proposed by Kingma and Welling as an approach to efficiently estimate the posterior inference. The aim of this method of inference is to approximate a joint distribution $Q(x;\theta)$ over a latent variable space x in order to approximate the true joint distribution $P(x)$ using the Kullback-Liebler Divergence to define "closeness". When this method of inference is utilized with the architecture of neural networks, the similarity to traditional autoencoders is the rough bottleneck design and the target class being the input itself. The similarities to autoencoders end there. The loss function used by a VAE includes the typical reconstruction loss such as mean squared error or smooth L1 loss as well as a divergence term for the approximate posterior being estimated.

Variational Bayes

A core problem in modern statistics is the approximation of complex probability densities. Bayesian statistics frame inferences as a calculation of the posterior. From the perspective of the core problem, this leads to Bayesian models that have difficult posteriors which need to be approximated.

One popular method of approximating the posterior is known as Markov Chain Monte Carlo (MCMC) Sampling. This method relies on repeat sampling given the prior and a likelihood function. Since this method inherently relies on the volume of samples for accuracy, the accuracy of the estimated posterior increases the longer the methods runs. A perfect MCMC model can be generated given infinite time which is not a viable solution

given real world resource restrictions.

This is where Variational Inference methods can be a more viable option. Variational Inference is a machine learning approach to solving these probability density approximations. When comparing Variational Inferencing (VI) to MCMC methods, it is noted that VI is faster and better at scaling with larger data than MCMC.

Variational Inference aims to use a latent variable space for optimizing conditional densities given a prior. Variational inference turns the approximation problem into an optimization problem by optimizing the fit of "variational parameters" in the latent distribution such that the KL divergence is minimized for the density of interest. The conditional density given an observed input variable x and the latent variable z is as follows:

$$p(z|x) = \frac{p(z, x)}{p(x)} \tag{2.10}$$

$$p(x) = \int p(z, x)dz \tag{2.11}$$

In order to calculate the $p(x)$ term, known as the *evidence*, the latent variables are reduced from the joint density shown in Eq. 2.11. This integral term is not always available in a closed form or is an exponential amount of time necessary to solve it. VI does not aim to solve this intractable solution but to find a lower bound to the term and optimize around the lower bound. A family of densities $\mathfrak{D}$ is specified over the latent variables with each $q(z) \in \mathfrak{D}$ being a candidate for approximating the conditional. The optimization is to minimize the KL divergence of the candidate and exact conditional. This amounts to

solving an optimization problem rather than an intractable integral.

$$q^*(z) = argmin_{q(z)\in\mathfrak{D}} KL(q(z)||p(z|x)) \tag{2.12}$$

Here $q^*(\cdot)$ is the optimum approximation of the conditional given the family of densities $\mathfrak{D}$. This solution still has a dependence on $\log p(x)$ from the KL divergence calculation, as shown below.

$$KL(q(z)||p(z|x)) = \mathbb{E}[\log q(z)] - \mathbb{E}[\log p(z|x)] \tag{2.13}$$

$$KL(q(z)||p(z|x)) = \mathbb{E}[\log q(z)] - \mathbb{E}[\log p(z,x)] + \log p(x) \tag{2.14}$$

Decomposing the KL divergence reveals an existing dependency on the evidence. Since this calculation is still intractable, optimization over a different objective that is equivalent to the KL divergence is performed. Declaring the $\log p(x)$ equivalent to a constant in Eq. 2.14 the negative KL divergence can be used as a lower bound of the evidence, this is dubbed the Evidence Lower Bound (ELBO).

$$ELBO(q) = \mathbb{E}[\log p(z,x)] - \mathbb{E}[\log q(z)] \tag{2.15}$$

$$ELBO(q) = \mathbb{E}[\log p(x|z)] - KL(q(z)||p(z)) \tag{2.16}$$

Equation 2.16 shows that the ELBO can be described as the combination of an expected

log likelihood and the KL divergence between the $p(z)$ prior and the $q(z)$ candidate. Dissecting the ELBO terms reveals how VI can optimize the placement of z values over this objective. The first term is the log likelihood of $q(z)$ mapping values to configurations in the latent variables that explain the observable data. The second term is the negative KL divergence of the candidate and the prior, this promotes densities that are similar to the prior. In this way, the objective is attempting to find a balance between likelihood and prior.

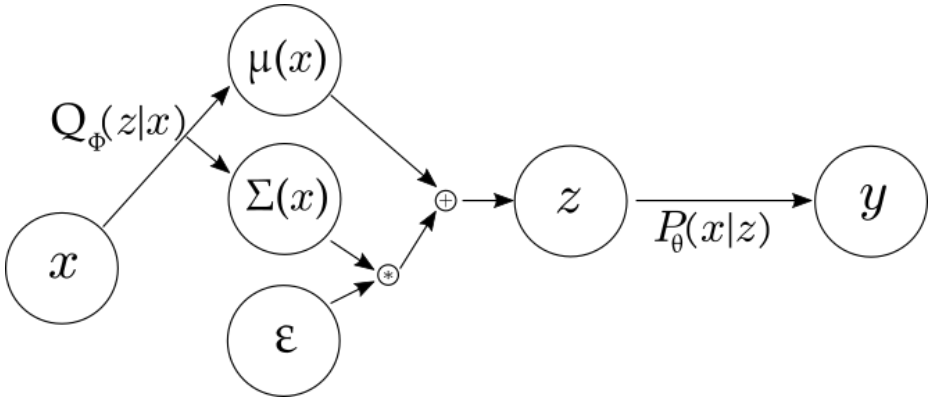

Figure 2.5: Kingma and Wellings' autoencoding variational Bayes method with the reconstruction term ϵ for backpropagation.

It is also a interesting that the first term in the ELBO equation 2.16 is the expected complete log likelihood which can be optimized by the Expectation Maximization (EM) algorithm. EM uses the fact the ELBO equation is the log likelihood ($\log p(x)$) when the candidate is the joint conditional, $q(z) = p(z|x)$. EM will be discussed in further detail in later sections. While EM assumes the $\mathbb{E}[\log p(z, x)]$ is tractable, a variational Bayes EM is possible where the expectation calculation is replaced with a lower bound on the marginal likelihood estimation over the latent variables and parameters.

Autoencoded Variational Bayes

Kingma and Welling introduced a practical estimator for the lower bound and its derivatives utilizing the neural network architecture of autoencoders. A approximate posterior in the form of $q_\phi(z|x)$ is assumed, though $q_\phi(z)$ can also be used if the estimator is not conditioned over x. Under certain conditions, for a chosen approximate posterior $q_\phi(z|x)$, the random variable z can be re-parameterized using the differential transformation $g_\phi(\epsilon, x)$ of auxiliary noise $\epsilon \sim N(0, I)$:

$$\tilde{z} = g_\phi(\epsilon, x) \quad \text{with} \quad \epsilon \sim p(\epsilon) \tag{2.17}$$

The appropriate selection of a distribution for $p(\epsilon)$ and function $q_\phi(\epsilon, x)$ will be discussed in a later section. For now, form Monte Carlo estimates of expectations of some function $f(z)$ w.r.t. $q_\phi(z|x)$:

$$\mathbb{E}_{q_\phi(z|x^i)}[f(z)] = \mathbb{E}_{p(\epsilon)}\Big[f(g_\phi(\epsilon, x^i))\Big] \simeq \frac{1}{L}\sum_{l=1}^{L} f(g_\phi(\epsilon^l, x^i)) \quad \text{where} \quad \epsilon^l \sim p(\epsilon) \tag{2.18}$$

Applying this technique to the variational lower bound (Eq. 2.16) yields Kingma and Welling's Stochastic Gradient Variational Bayes (SGVB) estimator.

Given an observation x, the inferred posterior distribution of the latent variable z is described by $q_\phi(z|x)$. The prior $p(z)$ is then assumed to be a isotropic unit Gaussian $p(z) \sim \mathcal{N}(0, I)$; a Bernoulli distribution is also commonly used [15]. The observational

model is then defined by a parametric distribution $p_\theta(x|z)$. This system is modeled using an autoencoder structure with the *encoder/inference* network learning ϕ and the *decoder/generative* network learning θ.

The objective of the VAE is to maximize the marginal likelihood of the observed x in expectation over the whole distribution of z.

$$\mathcal{D}_{vae}(\theta, \phi, x) = KL(q_\phi(z|x)||p_\theta(z)) \tag{2.19}$$

$$\tilde{\mathcal{L}}_{vae}(\theta, \phi, x) = \mathbb{E}_{q_\phi(z|x)}(\log p_\theta(x|z_i)) - \mathcal{D}_{vae} \tag{2.20}$$

The first term in Eq. 2.20 is the reconstruction accuracy of the network's output to the original input. The second term is the Kullback-Leibler divergence (KL), from Eq. 2.19, of the posterior to the prior, which acts as a regularizer. However, in order for back-propagation to be used on the variational parameters ϕ, z needs to be re-parameterized as a function of i.i.d noise (ϵ) and the output of the encoder network[15] shown in Eq. 2.21.

$$z = g_\phi(\epsilon, x) \tag{2.21}$$

$$\epsilon \sim \mathcal{N}(0, I) \tag{2.22}$$

β - Disentangled Representation

Research into disentanglement has become increasingly popular with the introduction of powerful generative methods such as VAEs and Generative Adversarial Networks (GANs).

The definition of disentanglement is closely related to the development of these methods, it is the process by which key aspects of the input data are encoded into specific latent dimensions. A simple example can be given where an input dataset consists of colorful geometric shapes of multiple sizes. A perfectly disentangled latent variable space would have a latent variable representing the color of the object, another variable would encode the shape present and another may map to the size of the shapes. By having a perfectly disentangled representation such as this, any possible color, shape and size combination could be generated with just these three latent variables. This aspect of reducing and isolating features to easily controlled variables drives current improvements in generative modeling. The stronger the encoded features are the more likely a meaningful sample can be generated from the network.

β-VAE is a modified VAE method for learning disentangled latent representations of data in an unsupervised manner [16]. The method introduces a hyperparameter β which weights the KL divergence term of the standard VAE ($\beta = 1$) objective as defined in Eq. 2.23. A disentangled representation is defined as one where single latent units are sensitive to changes in single generative factors, while being invariant to changes in others [17]. An example being a 3D object dataset where the learned disentangled latent variables encode the scale, orientation, color and object identity.

$$\mathcal{D}_{\beta-vae}(\theta, \phi, \beta, x) = \beta \cdot KL(q_\phi(z|x)||p_\theta(z)) \tag{2.23}$$

Varying β controls the regularization constraint on the network and can be viewed as

pressure to learn the disentangled representations [16]. A β-VAE with $\beta = 1$ is equivalent to the original VAE equation by Kingma and Welling [15]. Therefore, a $\beta > 1$ is key for applying pressure on the network during training. There is a trade-off between reconstruction accuracy and the quality of the representations in z with higher β values and so β must be optimized for the applied dataset and dimension of the z feature space.

Chapter 3

Proposed Method

This chapter outlines the proposed method of detecting and analyzing novel events using a β-VAE network with a GMM classifier. The chapter is organized as follows: first the data set collection method and organization are discussed, and the preprocessing methods used. The design of the β-VAE network is outlined and the GMM classifier is outlined as well. This classifier is composed of two parts, the latent classifier model and the projection of the model parameters to a different feature space for process variable processing. Finally, the model parameter mappings are outlined with the use of Lediot-Wolf covariance estimation in order to represent the GMM in the process variable space.

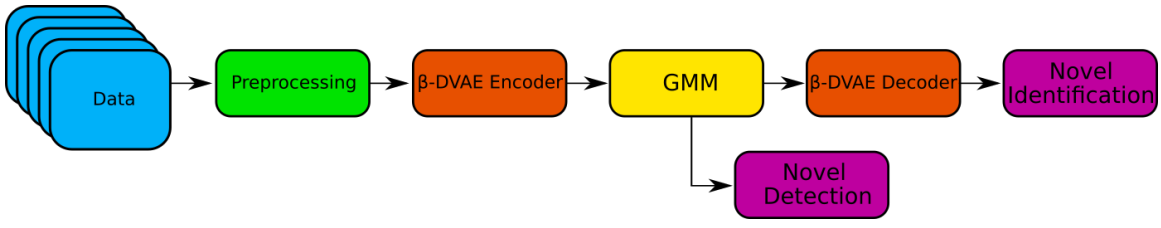

Figure 3.1: The System Overview for Novel Detection and Identification

Dataset

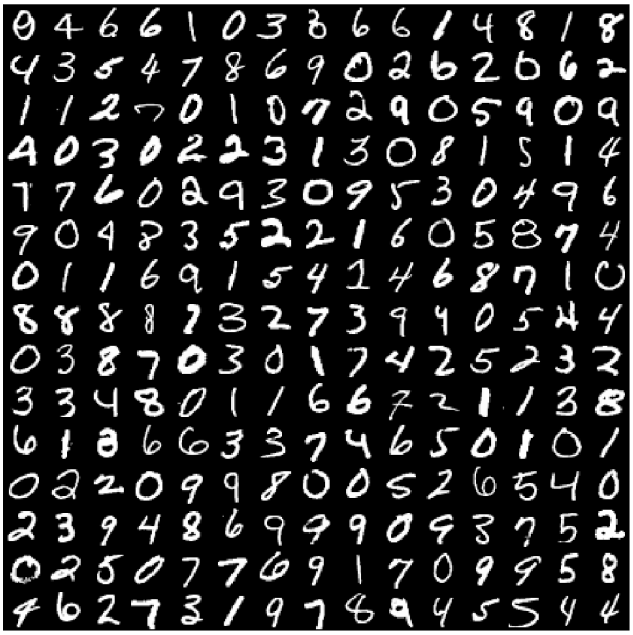

Figure 3.2: Data Samples from the MNIST Dataset.

In order to demonstrate the β-VAE network can operate as a standard classification method, as well as novel analysis, standard datasets were utilized to compare the β-VAE method to state-of-the-art classifiers. The two most common multivariate two-class datasets were selected from the UCI Machine Learning Repository [18], multi-class datasets can be used as well with one class being chosen as the target one-class. The cancer evaluation dataset, as well as the ionosphere testing datasets were chosen to compare classification performance. The MNIST handwriting dataset was also used as validation the β-VAE network was successful at encoding and reconstructing digits [19]. Table 3.1 outlines the

Table 3.1: Dataset names, sample counts, and class descriptions.

Dataset	# Attributes	# Target	# Non-Target	Target Label	Non-Target Label
Cancer	10	458	241	Benign	Malignant
Ionosphere	34	225	126	Good	Bad
MKS LVG3527A	35	279	899	Normal	F1,F2,F3
MKS LVG3560A	35	328	428	Normal	F1,F3

attributes, sample counts and target class for each dataset. In order to adhere to one-class classification techniques the target class chosen was the class most likely to represent *normal* conditions. For the cancer dataset the benign class was considered the target class and for the ionosphere data the "good" class was the target class. The state-of-the-art classifiers used for comparison were: k-Nearest Neighbor (k-NN) [20], Support Vector Machine with a radial basis kernel function (SVM-RBF) with Principal Component Analysis (PCA), and GMM with PCA [2]. These methods were chosen in order to compare simple methods such as k-NN, as well as methods similar to the proposed approach, such as SVM-RBF and GMM with PCA.

The primary dataset that was focused on in the experimental results was operational data collected from the MKS LVG3527A 27MHz RF generator and the MKS LVG3560A 60MHz generator [4][2]. Multivariate, time-series data, or fingerprints, were collected and provided by MKS ENI Products. These fingerprints were collected from generators during *normal* operating conditions during three different load conditions. The load conditions were *Fifty Ohms*, *Short* and *Open*. These conditions simulate full operational loads of the RF generators. Along with the known *normal* operational data, additional fingerprints were collected while generators were operating with 3 seeded faulty conditions; which are listed below:

1. Faulty Amplifier
2. Poor Solder Joints on Resistors
3. Poor Solder Joints on FETs

These *non-normal* conditions were chosen to closely mimic scenarios where the current quality control measures experience difficulty identifying *non-normal* operations. In order to evaluate the data, the fingerprints of each generator were partitioned into training, validation and testing. The *normal* fingerprints were split into 60% training and 20% validation and 20% testing while the *non-normal* fingerprints were separated 40/60% for validation and testing respectively.

Preprocessing

Before the data could go through the β-VAE network it needed to be processed in order to learn faster and more accurately. First the training data is rescaled to a maximum of $+1$ and a minimum of -1.

$$X_{scaled} = -2 \cdot \frac{X - min(X)}{max(X) - min(X)} + 1 \tag{3.1}$$

Then each variable has its mean subtracted in order to zero-mean the signals. All parameters of preprocessing are generated using the training data and are then used on the

validation and testing data for consistency.

β-DVAE Network

The β-DVAE model is designed with traditional VAE architecture in mind. It is comprised of a stochastic encoding network and a decoding network which maps inputs into a subspace z. The encoder has an initial denoising layer, this has intentionally been designed to be overcomplete since this has shown to produce better manifold learning. The level of noise injected can be controlled by a hyper parameter which modifies the magnitude and standard deviation of the Gaussian distribution the noise is generated from. The output of the denoising layer is the input to the stochastic encoding layer which produces a μ and Σ matrices. The z data is generated from sampling a Gaussian distribution defined by these μ and Σ terms. The dimension of these outputs is controlled by a hyper parameter, this parameter defines the size of the z variable and the final compression size of the input data. The z Term is then passed through two decoding layers which mirror the layer sizes of the inputs, one maps z to the overcomplete space while the second maps it to the reconstructed input space Y. Figure 3.3(a) shows the network topology and function mappings.

The network is trained using the DVAE objective function with the β parameter modifying the KL-divergence term. The KL-divergence takes the μ and Σ generated every mini-batch and calculates the derived Gaussian distribution's divergence from a predetermined distribution. For the purposes of this research, a zero mean and unit variance Gaussian has been chosen. The β term is multiplied into the KL-divergence to encourage meaningful

feature encoding in the z space. The reconstruction loss is also calculated then added to the KL-divergence term, this loss is determined by the mean squared error of the reconstructed Y and original input x. Figure 3.3(b) shows this loss calculation as a flow diagram.

$$\mathcal{D}_{\beta-dvae}(\theta, \phi, \beta, x) = \beta \cdot KL(\tilde{q_\phi}(z|\tilde{x})||p_\theta(z)) \tag{3.2}$$

$$\tilde{\mathcal{L}}_{\beta-dvae}(\theta, \phi, \beta, x) = \mathbb{E}_{p(z|\tilde{x})}(\log p_\theta(x|z_i)) - \mathcal{D}_{\beta-dvae} \tag{3.3}$$

The network can be trained using any standard optimization method such as Stochastic Gradient Descent, Adadelta or ADAM [21] as well as any additional forms of regularizing and batch control. All results reported will utilize minibatchs with ADAM optimization and no additional regularization techniques.

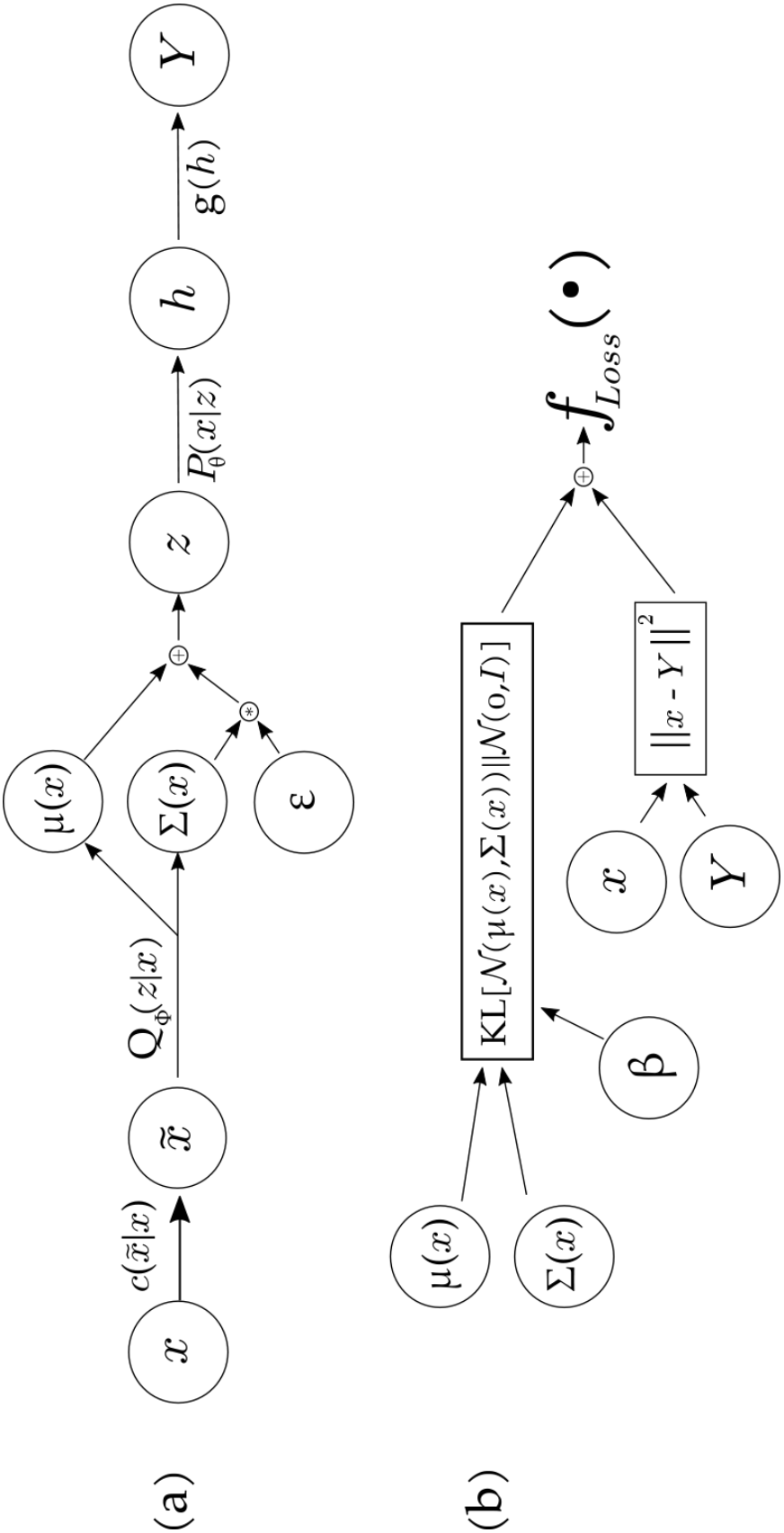

Figure 3.3: Proposed Method Process flow. The forward pass (a) and the loss calculation (b).

GMM Classification

Once the β-DVAE model has been trained and the input data is represented as latent variables, GMM learning and validation is performed. This method uses a k-component mixture of Gaussians to learn the model parameters. The model is built component-wise, applying expectation maximization (EM) until convergence [11]. The stopping criteria is a predefined number of components determined through choice or through a search algorithm for the k that maximizes the likelihood of the training data. From the training dataset the model parameters are as follows:

- $M(k \times q)$ - mean vectors of mixture.
- $C(q \times q)$ - covariance matrix of mixture.
- $W(k \times 1)$ - mixing weights.

Where k is the number of mixtures, and q is the number of features per sample in the dataset. The training data used to fit the mixtures contains only samples that have been labeled as *normal*. This ensures the learned GMM encompasses only the expected modes of operation and rejects all others.

The fitness of a sample with respect to the parameters of the model is quantified through the calculation of the likelihood that it's feature vector belongs to each component k. The log of the likelihood values for each k component is weighted by W and summed to determine the log-likelihood of the sample belonging to the mixture.

Classification using the learned model is achieved with one-class classification techniques. Since this approach assumes information is only available for the target class, a threshold is used to provide a binary decision [22]. This threshold is statistically determined after training. The threshold value is defined in Eq.2.5, where $\mu_{\mathcal{L}}$ and $\sigma_{\mathcal{L}}$ are the mean and variance of the log-likelihood of the training data. An additional parameter, λ, is used to parameterize the threshold for optimization.

Classifier Estimation in n-Dimensions

A majority of novel detection methods use a reduced dimension classification approach. However, while analyzing detected novel events in a latent data space is effective, most feature reduction methods abstract the relationship of input variables to latent variables making relating any analysis back to the original data space difficult. The learned mappings from the β-DVAE model can both embed inputs into a condensed feature space and relate the learned low dimensional classifier parameters back to the input data space. This allows a model trained in a low dimension to perform classification, then have its parameters related back to the original input space to provide per-variable likelihood analysis at the observable input level.

In order to map the classification model parameters to the original input dimension (n) using the β-DVAE transformations, any parameter that is defined as a point in the space can be mapped using the decoding network. For GMMs this means each component's means

can be easily related back to the process variable level seen in Eq. 3.4 and the mixture weights do not need mappings at all.

There can be a problem with mapping the covariance however, if the covariance is full, one where each component has a variance with every other component, or tied. A tied covariance can have the diagonal easily mapped without any issue however tied covariances are limiting and don't allow whole modeling of the data. In order to relate a full covariance to the process variable space the GMM must be sampled and the sample set remapped to the input space. Here the new full covariance can be estimated and the GMM can be reconstructed in the input space without having been learned there.

$$\hat{\mu}_k = W_{DAE-decoder} \cdot (W_{VAE-decoder} \cdot \mu_k + B_{VAE-decoder}) + B_{DAE-decoder} \tag{3.4}$$

Generating samples from a GMM is similar to sampling from a normal Gaussian, however, the mean and covariance components will be weighted by the mixing terms. This makes GMM a popular generative model for some tasks. A sample set must be large enough to be a good representation of the GMM or the resulting mapped covariance will impact classification performance. The sample set is mapped to the process variable space using the decoding stages of the β-DVAE network[13]. The new covariance can be estimated from these new samples in the input space. Classic empirical covariance calculations on large datasets such as this one can be unstable and result in unconditioned and un-invertible

matrix. Therefore, the Ledoit-Wolf covariance estimation is used in order to avoid any issues ensures a well-conditioned and invertible covariance matrix [23] [24].

With the GMM components in the process variable space the model can be applied as a classifier for novel detection as well as perform a per-component fitness estimation in order to highlight any individual components that are not performing as per the learned model.

Chapter 4

Results

Latent Model Results

The β-DVAE network was applied to the cancer, ionosphere, MNIST and MKS generator datasets. The network was trained in PyTorch on a Nvidia GTX-980 using an ADAM optimization on the gradients and Glorot-uniform initialization for all weights. Algorithm parameter selection was necessary for latent dimension size (z), the disentanglement term β, the number of mixtures (k) and the threshold term λ. A Grid search method was used in order to determine the optimal parameter values such that $z \in \{1, 2, 3, ..., 33\}$, $\beta \in \{1, 2, 3, ..., 17\}$, $k \in \{1, 2, 3, ..., 25\}$, $\lambda \in \{0.5, 1.0, 1.5, ..., 5.0\}$. The network was trained until the loss was stabilized to changes less than $1e^{-6}$.

An additional measure to verify the stability and consistency of the learned VAE mappings, the MNIS handwriting digit dataset was used to encode the $28x28$ grayscale images of the numbers 0 through 9. The training set was comprised of $60,000$ examples with all classes, the test data was $10,000$ digits. An example of the training digits is shown in figure 3.2. The samples were reshaped to $1x784$ vectors and were fed into the exact same network setup as the MKS with the input size modified to accommodate the larger input

vectors. The β parameter was then adjusted in order to show the effect that a higher value would have on the embedding of the data. The latent space was grid sampled and the sampled values were reconstructed into $28x28$ images and displayed for visualization of how the image aspects are varied over the latent space. Figure 4.1 displays the embedding plots and reconstructions.

For the classification datasets, training data was mapped to the latent space, where the GMM was trained with EM. Figure 4.2 displays an embedding of the MKS generator data into 2 latent dimensions with classification labels discerned by color. Classification results are reported as classification accuracy (ACC), true positive rate (TPR), and specificity (SPC) with standard deviations from 10 runs using the test data [25]. From Table 4.2, the GMM one class classifier trained on data encoded by the β-DVAE is comparable in performance to the state-of-the-art classifiers with classification accuracy within 2% on all datasets. The β-DVAE is as good as the GMM that was trained on data reduced by PCA, showing this is comparable to other one-class methods.

The two GMM approaches are compared using the true positive rates in Table 4.1. Since the true positive rate is an indication of how well a classifier models the learned class, it is a key criteria for evaluating one-class classifiers. By this criteria the β-DVAE is comparable to the GMM using PCA in both the latent dimension as well as the input dimension.

The size of the latent features was varied from 1 to the original input size 33 for both the

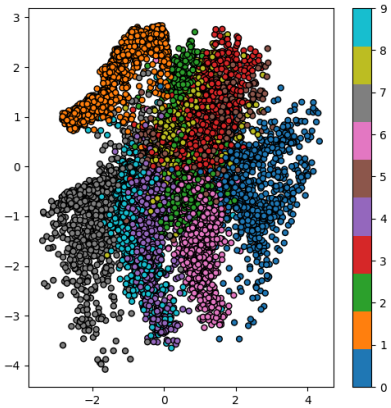

(a)

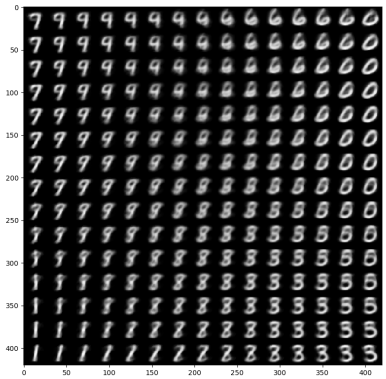

(b)

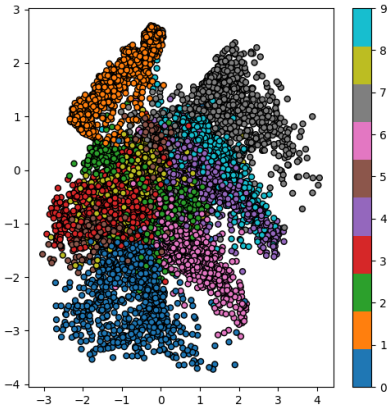

(c)

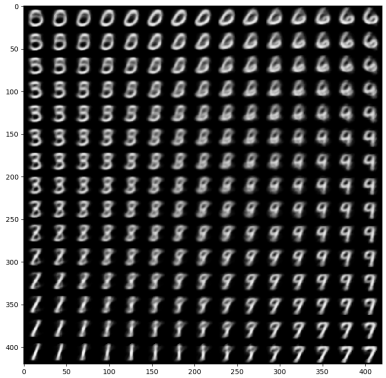

(d)

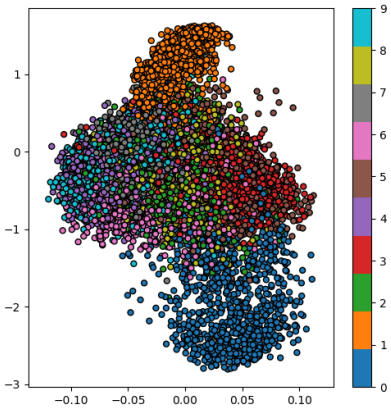

(e)

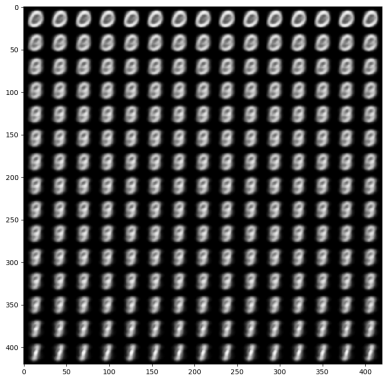

(f)

Figure 4.1: Latent 2D mapping of MNIST digits with reconstructed digits sampled from the latent space. (a)(b) $\beta = 1$, (c)(d) $\beta = 2$, (e)(f) $\beta = 7$

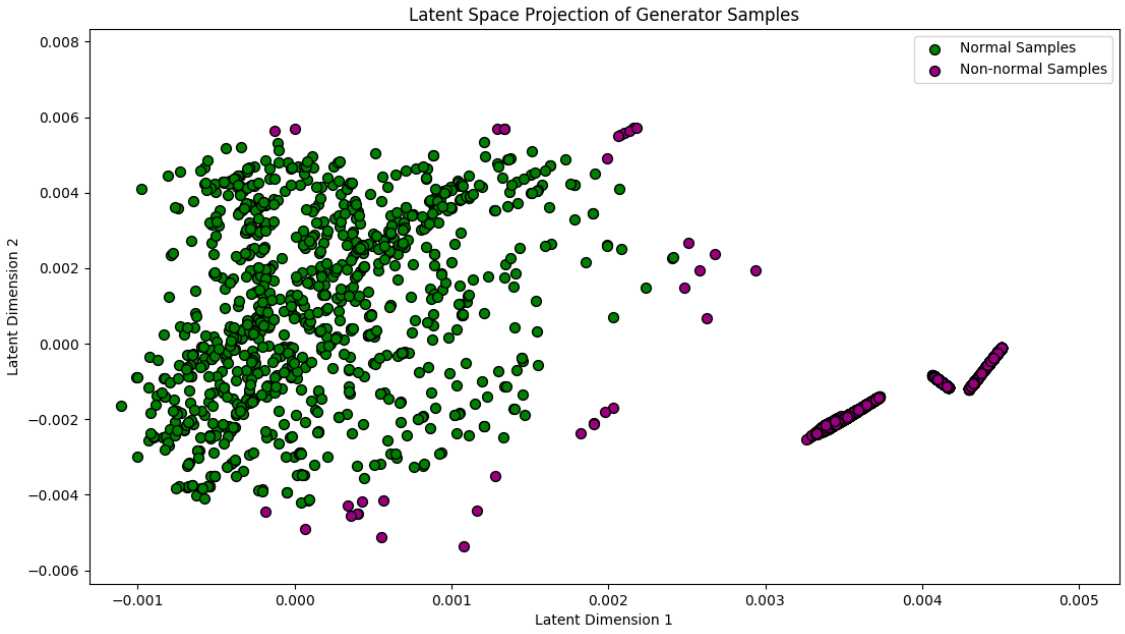

Figure 4.2: A 2D embedded view of MKS generator normal operation samples (green) and seeded faults (purple).

Table 4.1: One-Class Classification comparison of True Positive Rate of *normal* class.

Generator	β-DVAE-Latent	β-DVAE-Decoded	PCA_GMM
LVG3527A	97.31 (0.04)	97.21 (0.04)	98.54 (1.72)
LVG3560A	99.29 (0.01)	99.27 (0.01)	99.87 (0.50)

PCA and β-DVAE feature extraction methods. The results of the trained GMMs were taken over 10 trials for each feature size and displayed in Fig. 4.4 and 4.5. For both methods the GMM parameters were set similarly; $k = 3, \beta = 2$ and $\lambda = 2$. The PCA result takes longer to stabilize with smaller latent spaces and had a larger variance in performance at all levels compared to the β-DVAE mappings.

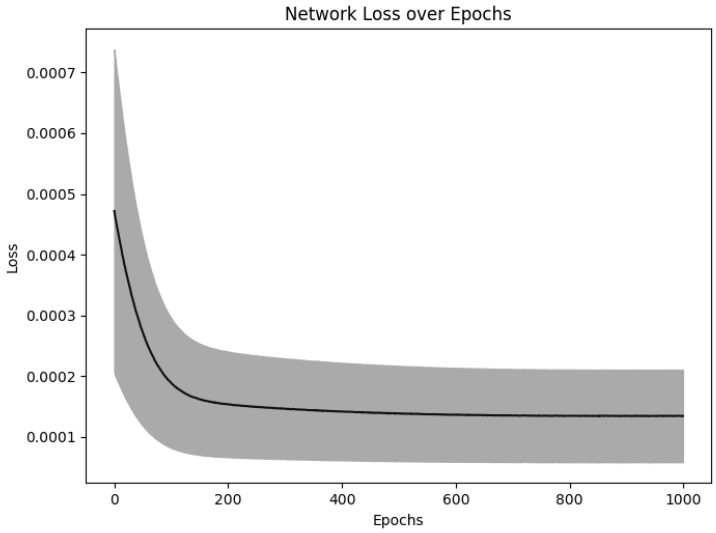

Figure 4.3: Network Loss during training over 1000 epochs. Mean squared error was used for the reconstruction loss and a β weighted KL divergence was added to the MSE loss.

Table 4.2: β-DVAE-GMM comparison with state-of-the-art classification methods [2]. Results are reported as mean per-class accuracy of 10 trials with standard deviation in parenthesis.

Dataset	k-NN	SVM-RBF	PCA-GMM	β-DVAE-GMM-Latent	β-DVAE-GMM-Decoded
Cancer	95.86 (1.11)	95.32 (1.94)	95.57 (1.26)	95.98 (1.21)	93.38 (2.63)
Ionosphere	85.88 (3.18)	87.52 (2.32)	88.51 (2.59)	90.99 (1.70)	87.44 (1.7)

Table 4.3: Number of mixtures, Accuracy, True Positive Rate and Specificity of Transformed GMMs. Results are reported as mean of 10 trials with standard deviation in parenthesis.

Dataset	Dim.	ACC	TPR	SPC	K	λ
Cancer	4	95.98 (1.21)	97.87 (1.01)	98.38 (0.38)	4	3
Cancer	8	93.38 (2.63)	92.86 (3.67)	92.63 (4.12)	4	3
Ionosphere	10	90.99 (1.41)	88.75 (0.59)	88.09 (0.93)	2	5
Ionosphere	34	87.44 (1.7)	82.29 (3.02)	78.02 (4.09)	2	5

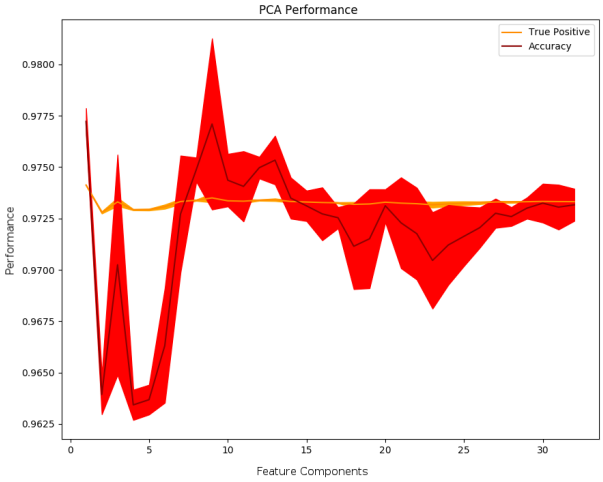

Figure 4.4: Performance Metrics accuracy and true positive rate of the GMM classification with PCA as the feature extractor. Results are reported as the mean of 10 trials while varying the number of PCA components used for features.

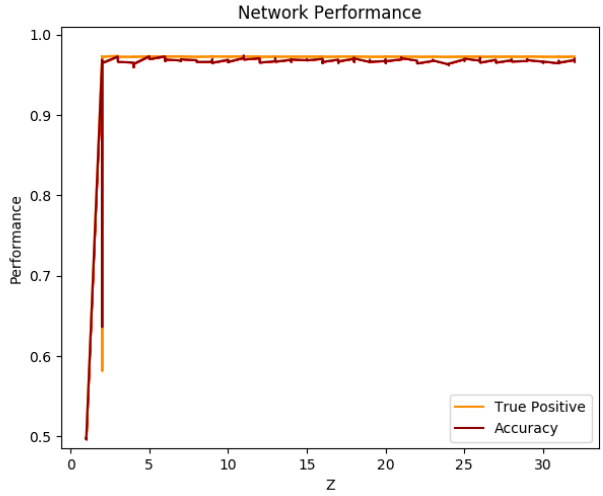

Figure 4.5: Performance Metrics accuracy and true positive rate of the GMM classification with β-DVAE Encoder network as the feature extractor. Results are reported as mean of 10 trials while varying the size of the encoded feature vectors.

Decoded Model Results

The trained GMM was then used to generate a new distribution at the input level by sampling points from the mixtures and applying the decoder network [13]. Distribution parameters were recalculated and a decision threshold was determined in the new space. The GMM in the latent space and the input space are compared across all performance measurements in Table 4.3. The transformed GMM has accuracy, true positive rates and specificity comparable to the GMM in the latent space. The transformed GMM is as effective as the latent GMM in classification.

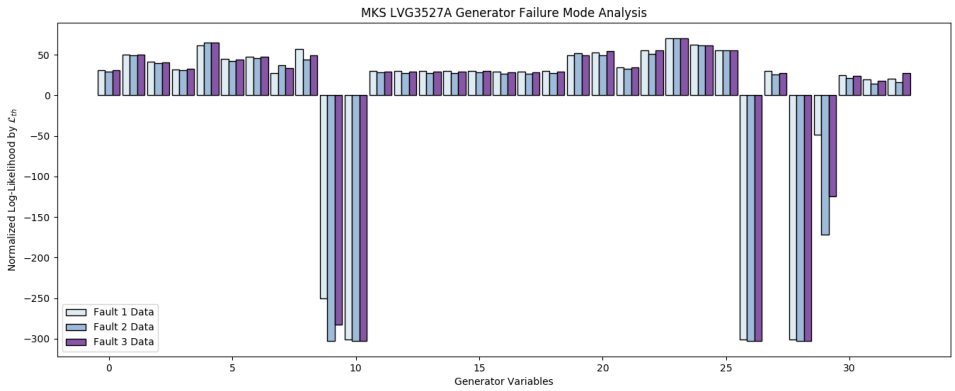

Figure 4.6: Per-variable likelihood analysis by the β-DVAE-Decoded model ($k = 3$) of three types of *non-normal* generator data. The log-likelihoods have been normalized by the threshold value indicated in order to emphasize variables that are *non-normal*.

The transformed mixture model allows for the log-likelihood calculation per-variable in order to analyze the fitness of that variable to a *normal* operation state. The system variables are listed in table 4.4. This analysis was applied to the three *non-normal* operational modes of the MKS LVG3527A generator. The log-likelihoods of each variable is shown in Figure 4.6 for each *non-normal* mode. From the analysis, it is easy to see how each

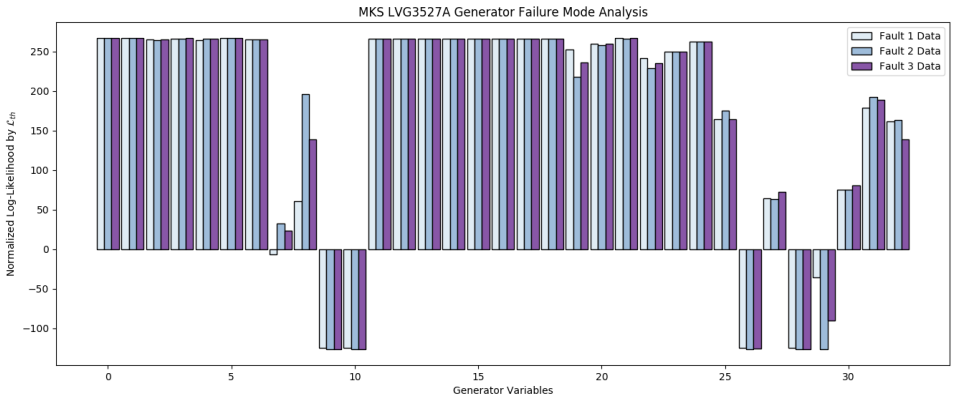

Figure 4.7: Per-variable likelihood analysis by the β-DVAE-Decoded model ($k = 8$) of three types of *non-normal* generator data. The log-likelihoods have been normalized by the threshold value indicated in order to emphasize variables that are *non-normal*.

fault responds across system inputs and which variables are most affected. A per-variable report such as this gives engineers and technicians who are repairing the generator an initial estimate of system variables affected and which was the most severe. This can prevent unnecessary part replacement and can provide a health-monitoring service for aging generators.

Table 4.4: MKS Generator System Variables, Environmental Variables, and Lifetime indicators for fault analysis.

Variable #	System Variable Name	Variable #	System Variable Name	Variable #	System Variable Name
1	Forward	13	PA02Current	25	PA Flange Temp
2	Reverse	14	PA03Current	26	Frequency
3	Dissipated	15	PA04Current	27	AC On Time
4	Drive Setpoint	16	PA05Current	28	AC Cycles
5	Rail Setpoint	17	PA06Current	29	RF On Time
6	GammaMagnitude	18	PA07Current	30	RF Cycles
7	GammaPhase	19	PA08Current	31	Contactor Closes
8	LifetimeForward	20	Fan Current	32	Fault Clears
9	LifetimeReverse	21	PA Voltage	33	Solenoid Cycles
10	LifetimeDissipated	22	Driver Current		
11	LifetimeDelivered	23	Ambient Air Temp		
12	PA01Current	24	Total PA Current		

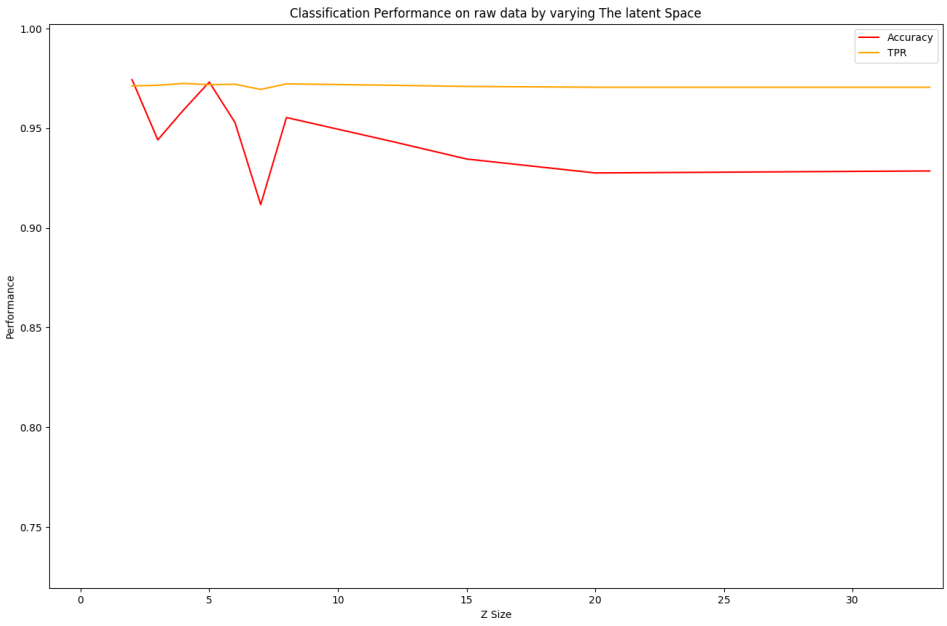

Figure 4.8: Decoded GMM model performance over varying sizes of the latent feature vector.

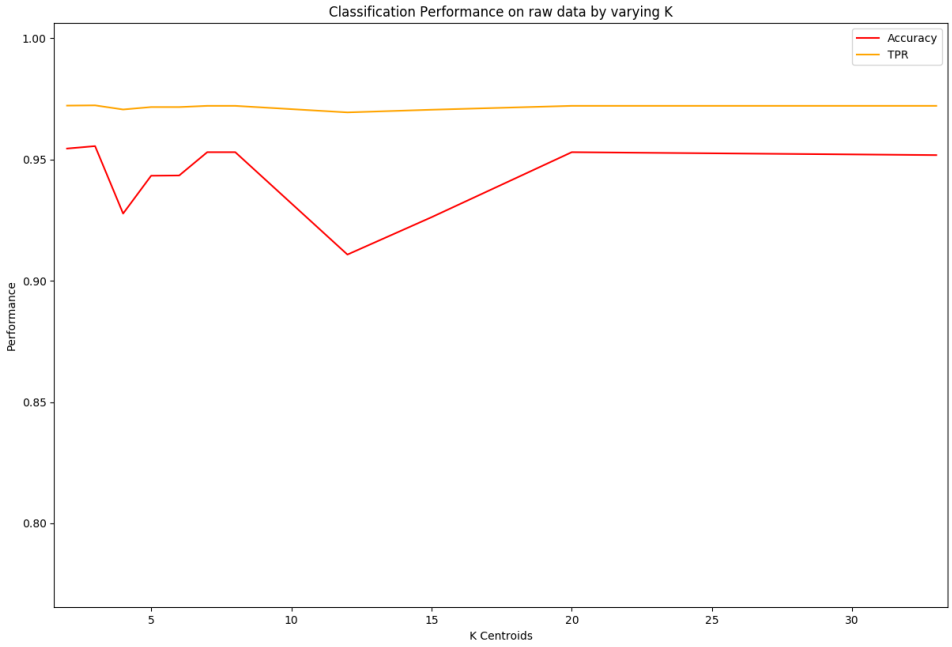

Figure 4.9: Decoded GMM model performance over varying values of K

Chapter 5

Conclusions

In this study, fault detection and identification were explored with the goal of utilizing the latent detection classifier in higher dimensions as a fault identification model. The dataset was collected from MKS Solutions from radio frequency plasma generators. It contained labeled samples that were representative of normal systems operation and three simulated faults. A β disentangled, denoising variational autoencoding neural network was created to encode the data to a latent feature space, as well as to decode the data back to a reconstructed input.

A one class classification method was implemented and trained on only data from the target class. Gaussian mixture models were selected due to their historical success as a fault detection approach. The performance of the feature extraction and classifier was compared to other state-of-the-art methods on standard datasets such as the cancer and ionosphere classification sets. The MKS data was then modeled and the classification results achieved a average accuracy of 97.31%.

The GMM parameters were decoded using the decoding network of the β-DVAE model and re-parameterized GMM performance was then compared to the state-of-the-art classifiers' performance. The decoded model was able to achieve an average accuracy of

97.21%. Finally, the fitness of the generator data was measured and evaluated against the fault events.

Chapter 6

Future Work

In this study, β disentanglement methods were used to increase feature encoding efficiency. There are many other methods of feature disentanglement including generative adversarial networks (GANs) and deep convolution inverse graphics networks (DC-IGN).

Testing other parametric classification methods such as k-means and Linear Discriminant Analysis with the presented reconstruction method can help to validate this research further.

Bibliography

[1] P. Vincent, H. Larochelle, Y. Bengio, and P.-A. Manzagol, "Extracting and composing robust features with denoising autoencoders," in *Proceedings of the 25th International Conference on Machine Learning*, ser. ICML '08. New York, NY, USA: ACM, 2008, pp. 1096–1103. [Online]. Available: http://doi.acm.org/10.1145/1390156.1390294

[2] R. M. Bowen, F. Sahin, and A. Radomski, "Systemic health evaluation of rf generators using gaussian mixture models," *Computers and Electrical Engineering*, vol. 53, no. Complete, pp. 13–28, 2016.

[3] S. J. Hong, W. Y. Lim, T. Cheong, and G. S. May, "Fault detection and classification in plasma etch equipment for semiconductor manufacturing *e*-diagnostics," *IEEE Transactions on Semiconductor Manufacturing*, vol. 25, no. 1, pp. 83–93, 2012.

[4] R. M. Bowen, F. Sahin, A. Radomski, and D. Sarosky, "Embedded one-class classification on rf generator using mixture of gaussians," in *2014 IEEE International Conference on Systems, Man, and Cybernetics (SMC)*, Oct 2014, pp. 2657–2662.

[5] J. Yu, "Semiconductor manufacturing process monitoring using gaussian mixture model and bayesian method with local and nonlocal information," *IEEE Transactions on Semiconductor Manufacturing*, vol. 25, no. 3, pp. 480–493, 2012.

[6] S. Mahadevan and S. L. Shah, "Fault detection and diagnosis in process data using one-class support vector machines," *Journal of Process Control*, vol. 19, no. 10, pp. 1627–1639, 2009.

[7] G. Chandrashekar and F. Sahin, "In-vivo fault prediction for rf generators using variable elimination and state-of-the-art classifiers," in *Systems, Man, and Cybernetics (SMC), 2012 IEEE International Conference on*. IEEE, 2012, pp. 1800–1805.

[8] G. Chandrashekar, F. Sahin, E. Cinar, A. Radomski, and D. Sarosky, "In-vivo fault analysis and real-time fault prediction for rf generators using state-of-the-art classifiers," in *Systems, Man, and Cybernetics (SMC), 2013 IEEE International Conference on*. IEEE, 2013, pp. 1634–1639.

[9] Y. Meidan, M. Bohadana, Y. Mathov, Y. Mirsky, D. Breitenbacher, A. Shabtai, and Y. Elovici, "N-baiot: Network-based detection of iot botnet attacks using

deep autoencoders," *CoRR*, vol. abs/1805.03409, 2018. [Online]. Available: http://arxiv.org/abs/1805.03409

[10] G. McLachlan and D. Peel, *Finite mixture models*. John Wiley & Sons, 2004.

[11] J. J. Verbeek, N. Vlassis, and B. Kröse, "Efficient greedy learning of gaussian mixture models," *Neural computation*, vol. 15, no. 2, pp. 469–485, 2003.

[12] D. P. Kingma, S. Mohamed, D. J. Rezende, and M. Welling, "Semi-supervised learning with deep generative models," in *Advances in Neural Information Processing Systems*, 2014, pp. 3581–3589.

[13] A. Creswell and A. A. Bharath, "Denoising adversarial autoencoders," *arXiv preprint arXiv:1703.01220*, 2017.

[14] D. J. Im, S. Ahn, R. Memisevic, Y. Bengio *et al.*, "Denoising criterion for variational auto-encoding framework." in *AAAI*, 2017, pp. 2059–2065.

[15] D. P. Kingma and M. Welling, "Auto-encoding variational bayes," *arXiv preprint arXiv:1312.6114*, 2013.

[16] I. Higgins, L. Matthey, A. Pal, C. Burgess, X. Glorot, M. Botvinick, S. Mohamed, and A. Lerchner, "beta-vae: Learning basic visual concepts with a constrained variational framework," 2016.

[17] Y. Bengio, A. Courville, and P. Vincent, "Representation learning: A review and new perspectives," *IEEE transactions on pattern analysis and machine intelligence*, vol. 35, no. 8, pp. 1798–1828, 2013.

[18] K. Bache and M. Lichman, "Uci machine learning repository," 2013.

[19] Y. Le Cun, B. Boser, J. S. Denker, D. Henderson, R. E. Howard, W. Hubbard, and L. D. Jackel, "Handwritten digit recognition with a back-propagation network," in *Proceedings of the 2Nd International Conference on Neural Information Processing Systems*, ser. NIPS'89. Cambridge, MA, USA: MIT Press, 1989, pp. 396–404. [Online]. Available: http://dl.acm.org/citation.cfm?id=2969830.2969879

[20] Y. Li and X. Zhang, "Diffusion maps based k-nearest-neighbor rule technique for semiconductor manufacturing process fault detection," *Chemometrics and Intelligent Laboratory Systems*, vol. 136, pp. 47–57, 2014.

[21] D. P. Kingma and J. Ba, "Adam: A method for stochastic optimization," *arXiv preprint arXiv:1412.6980*, 2014.

[22] D. M. J. Tax, "One-class classification: concept-learning in the absence of counter-examples [ph. d. thesis]," *Delft University of Technology, Stevinweg, The Netherlands*, 2001.

[23] O. Ledoit and M. Wolf, "Honey, i shrunk the sample covariance matrix," Department of Economics and Business, Universitat Pompeu Fabra, Economics Working Papers, 2003. [Online]. Available: https://EconPapers.repec.org/RePEc:upf:upfgen:691

[24] ——, "A well-conditioned estimator for large-dimensional covariance matrices," *Journal of Multivariate Analysis*, vol. 88, no. 2, pp. 365 – 411, 2004. [Online]. Available: http://www.sciencedirect.com/science/article/pii/S0047259X03000964

[25] C. E. Metz, "Basic principles of roc analysis," in *Seminars in nuclear medicine*, vol. 8, no. 4. Elsevier, 1978, pp. 283–298.